

# Image Inpainting with Markov Chains

Arpad Gellert\*, Remus Brad

Computer Science and Electrical Engineering Department, Lucian Blaga University of Sibiu,  
Emil Cioran Street, No. 4, 550025 Sibiu, Romania  
\*arpad.gellert@ulbsibiu.ro

**Abstract:** This paper presents a novel context-based image inpainting method. The proposed technique is applying Markov chains to restore the colors of objects from images affected by some external factors (like scratches or wipes) or partially covered by other objects. Thus, damages or unwanted objects can be removed from an image by replacing each pixel from such an area, based on the surrounding unaffected context information. Therefore, the restoration process is applied from the exterior to the interior, using for replacement colors occurring with the highest probability in similar contexts. Since we use context information, the proposed inpainting technique can successfully rebuild details in images. We have compared our method with other existing inpainting techniques and the results were better on some test images or comparable on others.

**Keywords:** Image processing, inpainting, context information, Markov chains, image restoration

## 1. Introduction

Inpainting is a technique which is replacing missing or affected parts from digital images or damaged films (regularly small areas). Three main categories of inpainting algorithms can be distinguished in the literature: structural, textural and combinations of both. All these methods are using the information from the unaffected areas in order to reconstruct the affected or missing areas. The structural inpainting is using geometrical operations to reestablish missing pixel colors. Textural inpainting algorithms are building up stochastic models based on the information from unaffected image areas and are using the obtained models to reconstruct the affected or missing areas, being thus able to restore textures, too. The combination of structural and textural inpainting in a hybrid approach, can exploit the advantage of both methods.

In this work, we are proposing a new context-based inpainting technique, which is relying on Markov chains to replace affected or missing image areas. The area which must be reconstructed is defined by the user through points, which are connected afterwards by lines. The reconstruction is started from the exterior of the affected area, with pixels whose context (consisting in the surrounding pixels) is at least partially in an unaffected

area. The unaffected context part is searched within a limited surrounding window. The affected or missing pixel is replaced with the color having the highest probability to occur in similar contexts or context parts. In the next iterations of the reconstruction process, the restored pixel colors can be used to restore other pixel colors. By using context information, the proposed method is appropriate to rebuild textures and details in images.

The rest of the paper is structured as follows. Section 2 presents the related work in image inpainting, while Section 3 describes in detail the proposed Markovian inpainting method. Section 4 presents the evaluation methodology and discusses the results and Section 5 concludes the paper, suggesting some possible further work directions.

## 2. Related Work

Inpainting algorithms classified on categories, have been presented in [24], [15] and in [7]. A stochastic model based on Markov random fields has been used in [6], where the algorithm is reconstructing texture by starting from one pixel. Similar contexts are queried by using the Sum of Squared Differences (SSD) similarity metric. One of the intensities surrounded by contexts determined as being similar is randomly chosen to replace missing pixel. In contrast with this work, we use the Sum of Absolute Differences (SAD) as similarity metric and we build up a Markov chain model using the current context and similar contexts situated in a limited surrounding area. We replace the missing pixel color with the most probable color discovered in similar contexts. Thus, our method can better rebuild textures.

In [2], the authors proposed an inpainting method which restores the marked area by continuing in the same angle the isophote lines that arrive to the boundaries of the region. An important disadvantage of their technique is that it cannot restore textures [4]. Therefore, in [3] the authors are combining the structural inpainting algorithm presented in [2] with the texture synthesis algorithm proposed in [6], the results of both operations contributing to reconstruct the image.

Another technique which can replicate both structure and texture has been presented in [5]. In the proposed exemplar-based inpainting method, the reconstruction process is performed in the order given by the priority

values computed for the patches along the fill front. High priority values are associated to the patches continuing strong edges and to the ones surrounded with high confidence pixels. The key difference between [5] and our work is that we apply pixel-level filling instead of patch-level filling. By focusing on a single pixel at each iteration of the algorithm, we expect to obtain better results. Exemplar-based inpainting using a locally linear neighbor embedding technique with low-dimensional neighborhood representation has been presented in [14]. In [1], the authors have analyzed the exemplar-based inpainting method from a variational viewpoint.

In [27], the authors presented a domain-based structural-aware image inpainting technique. They designed an iterative structure searching algorithm for structural restoration, by connecting the adjacent patches to form a repairing domain which assures coherency and accuracy.

In [17], the authors proposed an inpainting method for images containing textures with gradually changed illumination. Based on an energy function model of the problematic area, gradually modified from the center to the boundary, a gradually changed directional priority function is used for the gradual propagation of texture synthesis.

In [30], the authors combined a base reconstructor containing low-frequency information with a detail reconstructor containing high frequency information. The base layer can grasp the basic information, whereas the detail layer provides the local details. These two components are combined within a so-called base-detail generator.

In [23], the authors proposed an inpainting technique which extends the isotropic diffusion model with diffusion barriers provided by the user. An improved model was introduced in [16].

Convolutional neural networks have been applied for image inpainting in [19] and [26]. In [20] the authors applied partial convolution by using only unaffected pixel intensities. Region-wise convolution have been combined in [21] with non-local correlation among regions. In [29], the authors proposed a hybrid inpainting approach which combines convolutional neural networks and multi-scale neural patch synthesis. In [28], the authors presented a foreground-aware image inpainting system which learns to predict the foreground contour and inpaints the missing region based on the predicted contour. The contour completion is performed by combining a generator and a discriminator used to encourage the generator to provide sharp contours. The generator is a cascade of a coarse network and a refinement network.

### 3. Inpainting with Markov Chains

The first step requests to the user to select the image area wanted to be reconstructed. The selection is performed by clicking on different points onto the boundary of the target area. These selected points are stored in a list and connected by lines. All the pixels falling inside and on this polygon defined by the user are considered as belonging to the target area which must be reconstructed. The selection is depicted in Figure 1 on the

famous “cracked-plate” portrait of Abraham Lincoln, taken in 1865 by Alexander Gardner.

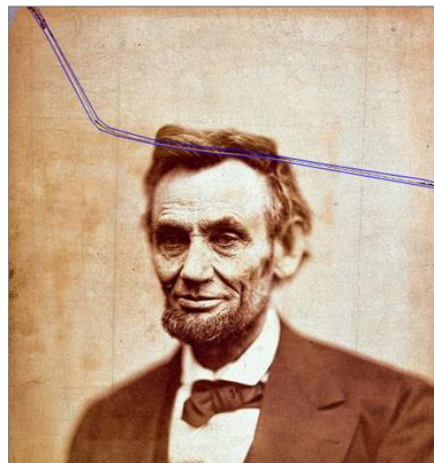


Fig. 1. Image area selection for inpainting on the photo of Abraham Lincoln.

The next step consists in using a stochastic method relying on Markov chains to reconstruct each pixel belonging to the selected target area. Markov chains can be used to determine the next probable value in a sequence, and have been successfully applied in bioinformatics [18], web mining [11], ubiquitous computing [8], speech recognition [22], image retrieval [25], image denoising [12], energy consumption modeling [13], etc. In a Markov chain of order  $R$ , the probability of the current state is depending on  $R$  previous states [10], as follows:

$$P[q_t | q_{t-1}, q_{t-2}, \dots] = P[q_t | q_{t-1}, \dots, q_{t-R}] \quad (1)$$

where  $q_t$  is the state of the Markov chain at time  $t$ . A general prediction method relying on Markov chains, applied on 1D sequence, was described in [9]. In [10] and [12], we repaired grayscale images affected by impulse noise using Markov chains adapted for pixel intensities from 2D image areas. Similarly with the current work, the probability of a pixel color in a context was determined as the number of its occurrences in similar contexts.

For the inpainting, we have adapted the application to be able to work with colors instead of grayscale intensities. Thus, the states are pixel colors. Further, we adopted the notations already established in the inpainting literature, denoting with  $\Omega$  the affected image area, with  $\delta\Omega$  the boundary of the affected area, with  $\Phi$  the search window and with  $\Psi_p$  the context of the replaceable pixel  $p_{x,y}$ .

In our proposed context based method, the affected pixel color  $p_{x,y}$  is replaced with the predicted color (next state). The unaffected surrounding pixel colors compose the context  $\Psi_p$  and the search window  $\Phi$  is encoding the previous states. The adjusted Markov model of order  $R$  is presented in (2), where  $CS$  is the size of the context  $\Psi_p$  (more exactly its width, see Figure 2),  $SD$  is the search distance (used to define the search window  $\Phi$ , as it is depicted in Figure 2),  $W$  is the width and  $H$  is the height of the image. As it can be observed, the color of a certain pixel  $p_{x,y}$  depends on the neighbor colors (the context).

$$P[p_{x,y} | p_{x+i,y+j} \notin \Omega, i, j = -SD, \dots, SD, 0 \leq x+i < W, 0 \leq y+j < H, \text{without } i=j=0] =$$

$$= P \left[ p_{x,y} \mid p_{x+i,y+j} \notin \Omega, i, j = -\frac{CS}{2}, \dots, \frac{CS}{2}, 0 \leq x+i < W, 0 \leq y+j < H, \text{without } i=j=0 \right] \quad (2)$$

The adjusted Markov model from (2) is illustrated in Figure 2, where the replaceable pixel from the center of the window is marked with red and the unaffected context pixels from its vicinity are marked with green. That context is searched within the surrounding window (limited by  $SD$  without leaving the image). All the pixel colors (marked with red in the top-left corner of Figure 2) which are situated in similar contexts (marked with green in the top-left corner of Figure 2) are considered as candidates to replace the color of the affected pixel. The similarity is determined based on the SAD metric. After the search process, the color of the affected pixel is replaced with the most frequent unaffected color found in similar image contexts (without leaving the image boundaries).

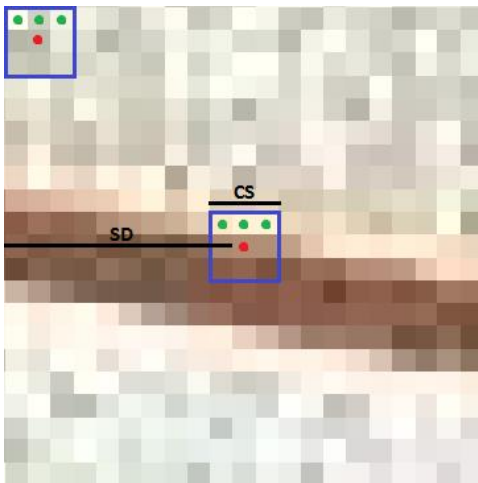


**Fig. 2.** Image inpainting with the Markov chain (on an area extracted from the photo of Abraham Lincoln).

The next pseudocode presents the Markov function which replaces a certain pixel  $p_{x,y}$  belonging to the affected area  $\Omega$ :

```
Markov(x, y, CS, SD, T)
  For i:=x-SD to x+SD, 0 ≤ i < W
    For j:=y-SD to y+SD, 0 ≤ j < H
      If (i=x AND j=y) OR Pixel(i, j) ∈ Ω then
        Continue
      If SAD(x, y, i, j, CS) < T then
        F[Color(i, j)] := F[Color(i, j)] + 1
  Return Max(F)
```

The input parameters of the above presented *Markov* function are: the row and the column of the current pixel, the search distance  $SD$ , the context size  $CS$  and the similarity threshold  $T$ . Inside the *for* instructions, we are searching for similar contexts, avoiding obviously the current one centered in  $x, y$ . The similarity degree measurement applied between the context of the replaceable pixel  $p$  and the contexts of the candidate pixels  $q$  is given in (3):

$$SAD = \sum_{j=0}^{CS-1} \sum_{i=0}^{CS-1} |\Psi_p(i, j) - \Psi_q(i, j)|, \text{without } i=j = \frac{CS}{2} \quad (3)$$

As lower the SAD value, as more similar the two compared contexts are. We have considered two contexts as being similar, if their SAD is less than  $T$ . The pseudocode of the SAD function, computing the similarity degree between two contexts, is defined as follows:

```
SAD(x1, y1, x2, y2, CS)
  S:=0
  For i:= -CS/2 to CS/2, 0 ≤ i+x1 < W, 0 ≤ i+x2 < W, do
    For j:= -CS/2 to CS/2, 0 ≤ j+y1 < H, 0 ≤ j+y2 < H do
      If i=0 AND j=0 then
        Continue
      S:=S + |I(i+x1, j+y1) - I(i+x2, j+y2)|
  Return S
```

The *for* instructions are summing the absolute differences between the pixels from the same position of the two contexts, avoiding the middle (which is not part of the context). The function can work with grayscale intensity (I) differences or with cumulative color component differences.

The frequencies of the unaffected pixel colors found in similar contexts are kept in  $F$ . The *Max* function returns the most frequent color which will be used to replace the color of the affected pixel  $p_{x,y}$ . The replacement is not performed if the *Markov* function fails finding similar contexts. Finally, the *Inpainting* function, which calls the *Markov* function, is given in the following pseudocode:

```
Inpainting(CS, SD, T)
  For each  $p_{x,y} \in \Omega$  do
    Set(x, y, Markov(x, y, CS, SD, T))
```

where the *Set* function is changing the color of  $p_{x,y}$  with the color returned by the *Markov* function.

#### 4. Evaluation

For a wider applicability and a higher processing speed, we have implemented our proposed inpainting method in a Windows Forms application, in C#.

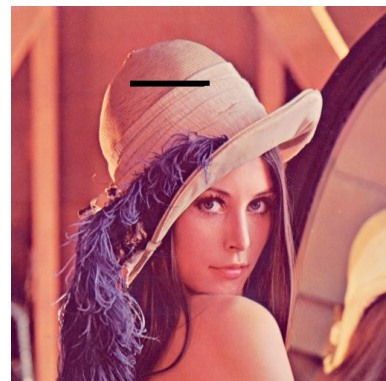


**Fig. 3.** Artificial defect of 849 pixels on the Lena image.

We performed the evaluations on the Lena, Peppers and Baboon color images, having artificial defects of different sizes. The defects were manually applied in arbitrary shape, size and position. Figure 3 presents an example of artificial defect (849 affected pixels) on the Lena image. We have also used in our evaluations the color photograph of Abraham Lincoln, mentioned earlier in this work.

The inpainting performance has been determined using the mean square error (MSE) and the peak signal-to-noise ratio (PSNR) metrics. The MSE is given in (4):

$$MSE = \frac{\sum_{i=0}^{W-1} \sum_{j=0}^{H-1} (R(i, j) - O(i, j))^2}{W \cdot H} \quad (4)$$

where  $W$  and  $H$  are the image width and height,  $R$  is the repaired image and  $O$  is the original (obviously unaffected) image. The goal is to obtain low MSE values. The PSNR computation is presented in (5):

$$PSNR = 10 \cdot \log_{10} \frac{255^2}{MSE} \quad (5)$$

Our goal is to obtain high PSNR values. The MSE can be computed based on the PSNR values as follows:

$$MSE = 255^2 \cdot 10^{-\frac{PSNR}{10}} \quad (6)$$

The proposed Markov inpainting model has been configured step by step on the Lena, Peppers and Baboon test images. First, we have varied the  $SD$  parameter (and thus implicitly the size of the search window  $\Phi$ ), by maintaining  $CS$  on 3, and  $T$  on 300. The MSE and PSNR measurements are presented in Figures 4 and 5, respectively. It can be observed that the best  $SD$  value is 5. Lower values than 5 are not feasible since the search window  $\Phi$  would be too small, with fewer chances to find the searched context. On the other hand, with high  $SD$  values, the search window  $\Phi$  would be too large and not specific to the target area  $\Omega$  which must be repaired.

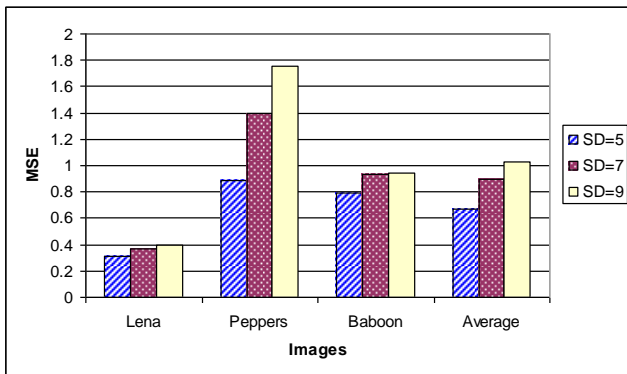


Fig. 4. MSE by varying  $SD$  with fixed  $CS=3$  and  $T=300$ .

Next, we have varied the value of the  $CS$  parameter, by fixing the  $SD$  on 5 and still maintaining  $T$  on the initial

value 300. The obtained MSE and PSNR values are depicted in Figures 6 and 7, respectively. As we can see, the best evaluated  $CS$  value is 7. Higher  $CS$  values would increase the processing time and would also reduce the chances to find a large context in a small search window  $\Phi$ , already fixed in the previous step by  $SD=5$ .

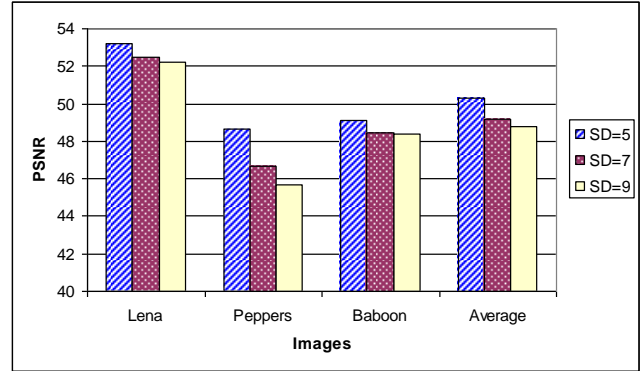


Fig. 5. PSNR by varying  $SD$  with fixed  $CS=3$  and  $T=300$ .

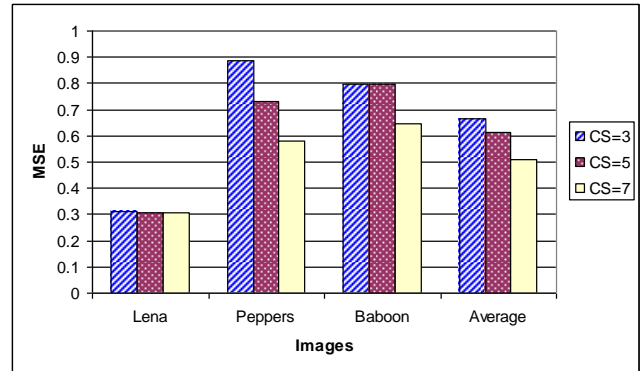


Fig. 6. MSE by varying  $CS$  with fixed  $SD=5$  and  $T=300$ .

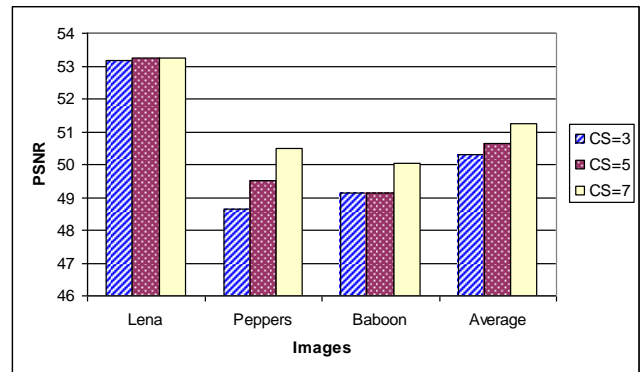


Fig. 7. PSNR by varying  $CS$  with fixed  $SD=5$  and  $T=300$ .

The next varied parameter is the similarity threshold  $T$ . The MSE and PSNR measurements presented in Figures 8 and 9, respectively, were obtained by fixing the  $SD$  on 5 and the  $CS$  on 7. We can observe that the initial threshold value ( $T=300$ ) was the optimal. Higher values of  $T$  are increasing the MSE and are decreasing the PSNR. In comparison with the value obtained in [10] and [12] for the same parameter  $T$  in image denoising, the optimal value 300 obtained here is reasonable, taking into account that

the context is quite large. We have tried also lower values for  $T$ , but with poor inpainting results, since the lower similarity threshold implies the necessity of finding contexts with low SAD values, which is often impossible.

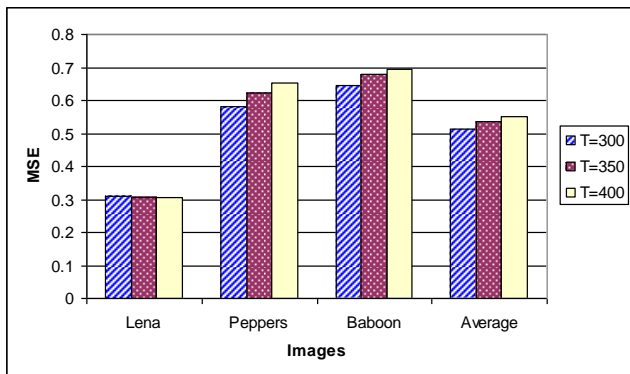


Fig. 8. MSE by varying  $T$  with fixed  $SD=5$  and  $CS=7$ .

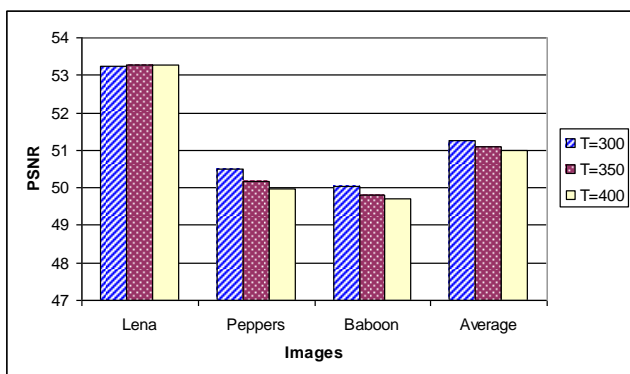


Fig. 9. PSNR by varying  $T$  with fixed  $SD=5$  and  $CS=7$ .

Figure 10 presents the Lena image after the Markovian inpainting of the artificial defect presented in Figure 3. One can observe that the artificial defect was very well replaced.



Fig. 10. The Lena image with artificial defect of 849 pixels after Markovian inpainting.

Next, we will use this optimal configuration of our inpainting algorithm for comparisons with other existing techniques, in terms of MSE and PSNR. Figures 11 to 16 are presenting comparatively our Markov inpainting method ( $SD=5$ ,  $CS=7$ ,  $T=300$ ) and the techniques developed by Bertalmio et al. [2], Oliveira et al. [23], Hadhoud et al. [16], Efros et al. [6] and Criminisi et al. [5], described in Section 2. As the comparative evaluations show, our proposed Markov inpainting method clearly outperforms all the other techniques on the Lena test image on all mask sizes (see Figures 11 and 12). On the Peppers test image, it is better than all the other techniques on high mask size and provides similar results on low and medium mask sizes (see Figures 13 and 14). On the Baboon image, it is better than the methods developed by Oliveira et al., Hadhoud et al. and Criminisi et al. on high mask size and is similar with the method of Hadhoud et al. on low and medium mask sizes (see Figures 15 and 16).

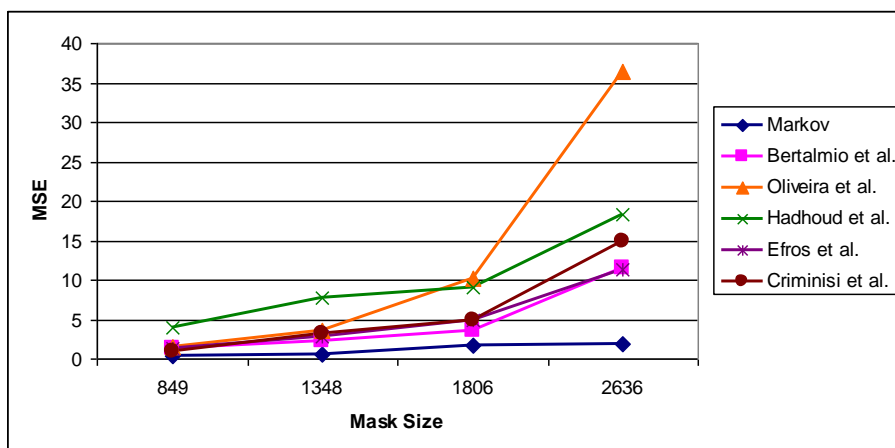


Fig. 11. Comparing the MSE of our optimal Markov inpainting method with other existing techniques on the Lena image.

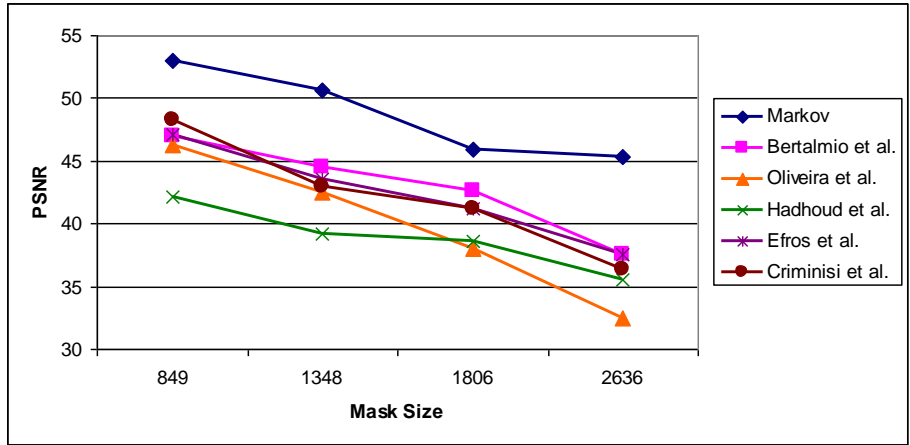


Fig. 12. Comparing the PSNR of our optimal Markov inpainting method with other existing techniques on the Lena image.

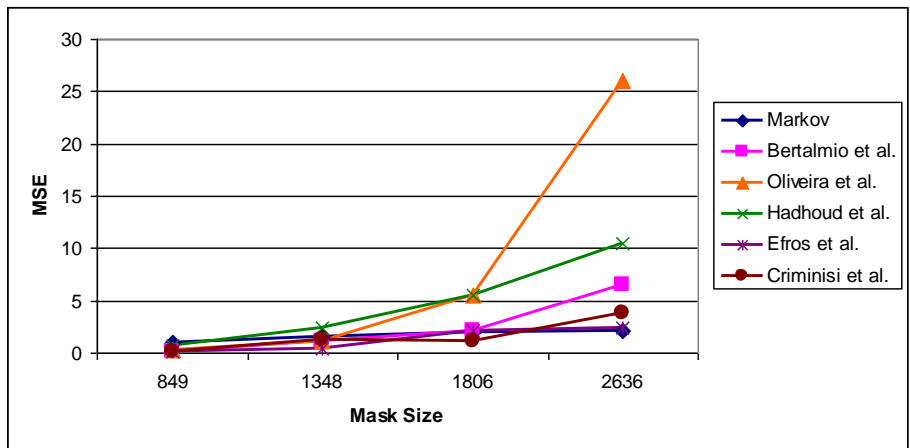


Fig. 13. Comparing the MSE of our optimal Markov inpainting method with other techniques on the Peppers image.

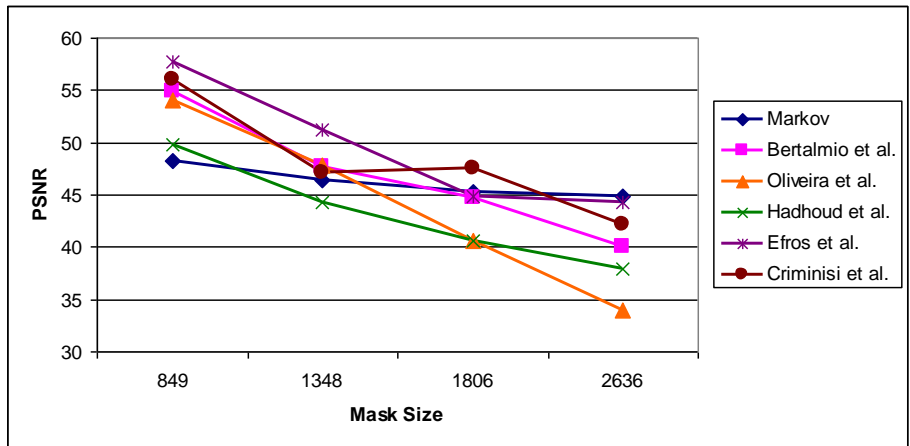


Fig. 14. Comparing the PSNR of our optimal Markov inpainting method with other techniques on the Peppers image.

Finally, we present the result of our inpainting method on the photograph of Abraham Lincoln. As Figure 17 shows, the crack could be successfully removed, being replaced with highly reliable colors. Some details in the

background, but also in Lincoln's hair, were very well reconstructed due to the context information used by our method.

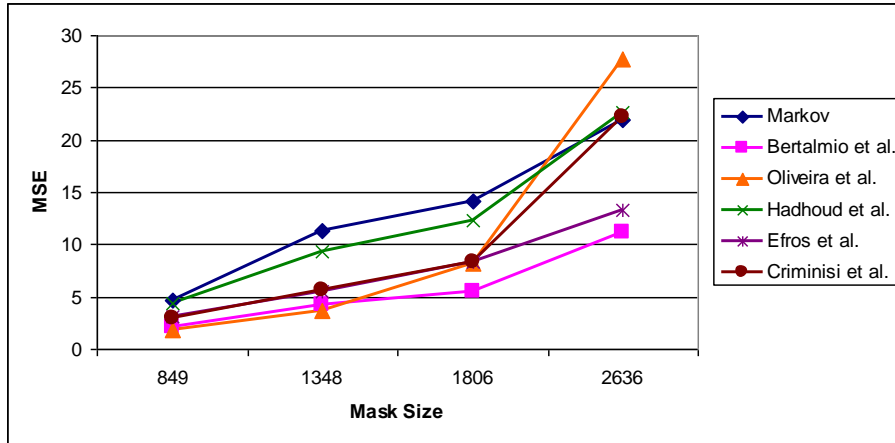


Fig. 15. Comparing the MSE of our optimal Markov inpainting method with other techniques on the Baboon image.

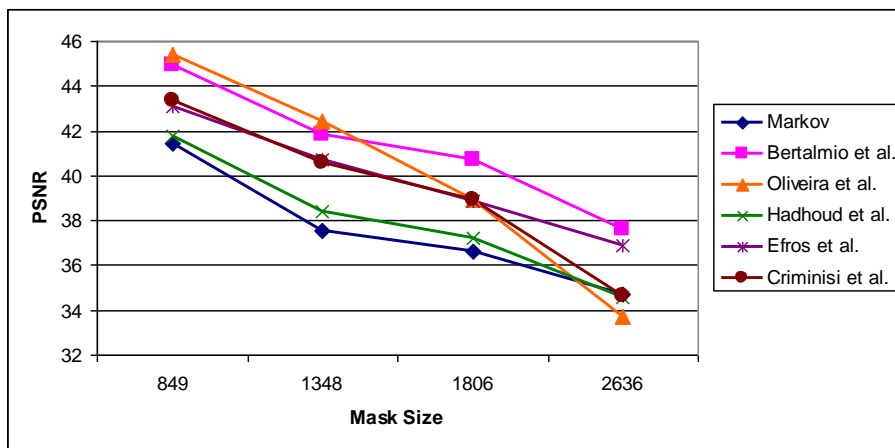


Fig. 16. Comparing the PSNR of our optimal Markov inpainting method with other techniques on the Baboon image.

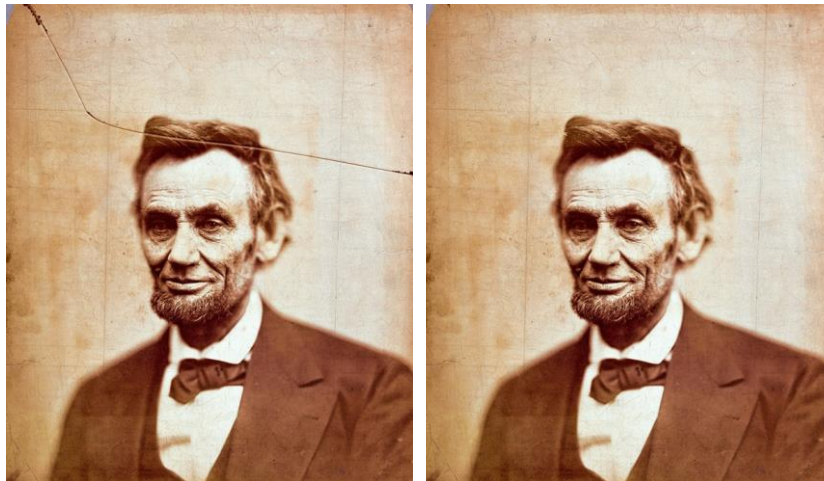


Fig. 17. Markovian inpainting on the photo of Abraham Lincoln (the original on left, the repaired one on right).

## 5. Conclusions and Further Work

In this work, we introduced a new contextual inpainting method which is using Markov chains in order to repair pixel colors from images affected by external factors or to replace pixel colors belonging to image areas covered by objects or texts. The user must select the target (replaceable) area. Our inpainting algorithm is replacing each pixel from the target area based on the surrounding

unaffected context information. Therefore, the restoration process is applied from the exterior to the interior within the selected target area. For the replacement of a certain pixel, we explored a limited surrounding image area to identify the color occurring with the highest probability in similar contexts. Since we use context information, the proposed inpainting technique can very well rebuild the image details. We have determined in our experiments the best parametrical configuration of the proposed Markov

inpainting technique consisting in a context size of 7, a search distance of 5 and a similarity threshold of 300. We have compared our optimally configured method with other existing inpainting techniques and the results were better on some test images and comparable on others. The results obtained on the famous “cracked-plate” portrait of Abraham Lincoln, were remarkable.

In our opinion, this new inpainting method still has a good future development potential. As a further work direction, we intend to integrate our context-based technique, together with a structural one, into a hybrid inpainting method.

## Acknowledgements

We thank our former BSc student Andrei Cojanu for providing his help in adapting the Markov filter.

## References

1. Aujol, J., Ladjal, S., Masnou, S.: ‘Exemplar-based inpainting from a variational point of view’, *SIAM Journal on Mathematical Analysis*, 42, (3), 2010, pp. 1246–1285.
2. Bertalmio, M., Sapiro, G., Caselles, V., Ballester, C.: ‘Image inpainting’, 27th Annual Conference on Computer Graphics and Interactive Techniques, New Orleans, LA, USA, July 2000, pp. 417–424.
3. Bertalmio, M., Vese, L., Sapiro, G., Osher, S.: ‘Simultaneous structure and texture image inpainting’, *IEEE Transactions on Image Processing*, 12, (8), 2003, pp. 882–889.
4. Bugeau, A., Bertalmio, M., Caselles, V., Sapiro, G.: ‘A Comprehensive Framework for Image Inpainting’, *IEEE Transactions on Image Processing*, 19, (10), 2010, pp. 2634–2645.
5. Criminisi, A., Pérez, P., Toyama, K.: ‘Region Filling and Object Removal by Exemplar-Based Image Inpainting’, *IEEE Transactions on Image Processing*, 13, (9), 2004, pp. 1200–1212.
6. Efros, A., Leung, T.: ‘Texture Synthesis by Non-parametric sampling’, 7th IEEE International Conference on Computer Vision, Corfu, Greece, September 1999, pp. 1033–1038.
7. Elharrouss, O., Almaadeed, N., Al-Maadeed, S., Akbari, Y.: ‘Image Inpainting: A Review’, *Neural Processing Letters*, 2019.
8. Gellert, A., Vintan, L.: ‘Person Movement Prediction Using Hidden Markov Models’, *Studies in Informatics and Control*, 15, (1), National Institute for Research and Development in Informatics, Bucharest, March 2006, pp. 17–30.
9. Gellert, A., Florea, A.: ‘Investigating a New Design Pattern for Efficient Implementation of Prediction Algorithms’, *Journal of Digital Information Management*, 11, (5), 2013, pp. 366–377.
10. Gellert, A., Brad, R.: ‘Context-Based Prediction Filtering of Impulse Noise Images’, *IET Image Processing*, 10, (6), June 2016, pp. 429–437.
11. Gellert, A., Florea, A.: ‘Web Prefetching through Efficient Prediction by Partial Matching’, *World Wide Web: Internet and Web Information Systems*, 19, (5), September 2016, pp. 921–932.
12. Gellert, A., Brad, R.: ‘Studying the influence of search rule and context shape in filtering impulse noise images with Markov chains’, *Signal, Image and Video Processing*, 12, (2), February 2018, pp. 315–322.
13. Gellert, A., Florea, A., Fiore, U., Palmieri, F., Zanetti, P.: ‘A study on forecasting electricity production and consumption in smart cities and factories’, *International Journal of Information Management*, 49, 2019, pp. 546–556.
14. Guillemot, C., Turkan, M., Le Meur, O., Ebdelli, M.: ‘Image Inpainting using LLE-LDNR and Linear Subspace Mappings’, 38th IEEE International Conference on Acoustics, Speech, and Signal Processing, Vancouver, Canada, May 2013, pp. 1558–1562.
15. Guillemot, C., Le Meur, O.: ‘Image inpainting: overview and recent advances’, *IEEE Signal Processing Magazine*, 31, (1), 2014, pp. 127–144.
16. Hadhoud, M.M., Moustafa, K.A., Shenoda, S.Z.: ‘Digital Images Inpainting using Modified Convolution Based Method’, *Optical Pattern Recognition XX*, 7340, 2009.
17. He, K., Shen, C.-N., Niu, J.-H., Huang, W.-R.: ‘Effective inpainting method for natural textures with gradually changed illumination’, *Signal, Image and Video Processing*, 13, 2019, pp. 69–77.
18. Jääskinen, V., Parkkinen, V., Cheng, L., Corander, J.: ‘Bayesian clustering of DNA sequences using Markov chains and a stochastic partition model’, *Statistical Applications in Genetics and Molecular Biology*, 13, (1), February 2014, pp. 105–121.
19. Laube, P., Grunwald, M., Franz, M.O., Umlauf, G.: ‘Image Inpainting for High-Resolution Textures using CNN Texture Synthesis’, *Computer Graphics & Visual Computing*, Swansea, UK, 2018.
20. Liu, G., Reda, F., Shih, K., Wang, T.-C., Tao, A., Catanzaro, B.: ‘Image Inpainting for Irregular Holes Using Partial Convolutions’, *European Conference on Computer Vision*, Munich, Germany, 2018, pp. 85–100.
21. Ma, Y., Liu, X., Bai, S., Wang, L., He, D., Liu, A.: ‘Coarse-to-Fine Image Inpainting via Region-wise Convolutions and Non-Local Correlation’, 28th International Joint Conference on Artificial Intelligence, Macao, China, 2019, pp. 3123–3129.
22. Mushtaq, A., Lee, C.-H.: ‘An Integrated Approach to Feature Compensation Combining Particle Filters and Hidden Markov Model for Robust Speech Recognition’, *IEEE International Conference on Acoustics, Speech, and Signal Processing*, Kyoto, Japan, 2012, pp. 4757–4760.
23. Oliveira, M.M., Bowen, B., McKenna, R., Chang, Y.-S.: ‘Fast digital image inpainting’, *Proceedings of the International Conference on Visualization, Imaging and Image Processing*, Marbella, Spain, 2001, pp. 261–266.
24. Patel, P., Prajapati, A., Mishra, S.: ‘Review of Different Inpainting Algorithms’, *International Journal of Computer Applications*, 59, (18), 2012, pp. 30–34.
25. Waghchawre, A.J., Shinde, J.V.: ‘Query Mining for Image Retrieval System Using Markov Chain Model’, *International Conference on Emerging Trends in Computer Engineering, Science and Information Technology*, India, 2015, pp. 109–112.
26. Wang, Y., Tao, X., Qi, X., Shen, X., Jia, J.: ‘Image Inpainting via Generative Multi-Column Convolutional Neural Networks’, 32nd Conference on Neural Information Processing Systems, Montréal, Canada, 2018.
27. Wei, Y., Liu, S.: ‘Domain-based structure-aware image inpainting’, *Signal, Image and Video Processing*, 10, (5), 2016, pp. 911–919.
28. Xiong, W., Yu, J., Lin, Z., Yang, J., Lu, X., Barnes, C., Luo, J.: ‘Foreground-Aware Image Inpainting’, 2019 IEEE Conference on Computer Vision and Pattern Recognition, Long Beach, CA, USA, 2019.
29. Yang, C., Lu, X., Lin, Z., Shechtman, E., Wang, O., Li, H.: ‘High-Resolution Image Inpainting using Multi-Scale Neural Patch Synthesis’, 2017 IEEE Conference on Computer Vision and Pattern Recognition, Honolulu, HI, USA, 2017.
30. Zhang, R., Ren, Y., Qiu, J., Li, G.: ‘Base-Detail Image Inpainting’, 30th British Machine Vision Conference, Cardiff, UK, 2019.